Pergamon

Bioorganic & Medicinal Chemistry 6 (1998) 465–472

BIOORGANIC & MEDICINAL CHEMISTRY

Structural Study on Silkworm Eclosion Hormone Fragment (1–34) in Solution by Proton Nuclear Magnetic Resonance Spectroscopy

Atsuko Y. Nosaka,* Kenji Kanaori,† Ichiro Umemura, Michihiro Takai and Norihisa Fujita‡

[a]*International Research Laboratories, Ciba–Geigy Japan Ltd., P.O. Box 1, Takarazuka 665, Japan*

Received 26 September 1997; accepted 21 November 1997

Abstract—Eclosion hormone (EH) is a neuropeptide hormone which controls the ecdysis behavior in insect. The three dimensional structure of the N-terminal fragment (1–34) of the eclosion hormone which was predicted to contain a compact region crucial for the EH activity was studied in 50% d_3-trifluoroethanol(TFE)/50% H_2O at pH 3 and 298 K by ^1H NMR spectroscopy with the combined use of distance geometry and molecular dynamics calculations. NMR results indicated that the fragment actually assumes an α-helix between Ala10 and Gln20, but no rigid structure is present from Cys21 through the C-terminus and for the N-terminal region (Ser1–Asp9). The elucidated structure was compared with the predicted structure of the native EH for the further development of the design of the insecticide.

Introduction

Eclosion hormone (EH) is an insect neuro-secretory hormone which triggers the sequential performance of pre-ecdysis (cuticle loosing) and ecdysis (cuticle shedding) behavior of insects.[1] EHs were purified from *Bonbyx mori*[2] and *Manduca sexta*,[3,4] by three groups independently, and turned out to be peptide hormones which are comprised of single amino acid chains of 62 residues. Six cysteines are well conserved in the two species and can form three disulfide bonds (Figure 1) which are required for biological activity.[5] Various lines of evidence indicate that EH acts on its receptor and causes rapid turnover of phospholipids which induce an accumulation of cGMP.[6–10] The increase in cGMP subsequently activates a cGMP-dependent protein kinase which in turn phosphorylates a certain protein, EGP (the EH and cGMP-stimulated phosphoprotein). EGPs play an important role in the ecdysis behavior.[11] EHs distribute in a wide variety in invertebrate but not in vertebrate species.[12,13] Because of this restricted distribution of the peptide in insects, this polypeptide has been intensively investigated with the aim of development of a new type of insecticide which could act on the EH receptor and interfere with the insect eclosion behavior. The information of the precise tertiary structure of EH is desirable to assist in probing appropriate direction for the design of the inhibitor. However, few studies have been reported on these problems so far.[5,14] Recently, Kikuchi et al.[14] have identified Glu12, Met24 and Phe25 as important residues for the EH action by means of the Gly substitution method.[15] They predicted the existence of three short range compact regions, i.e., Asp9–Met24, Trp28–Glu30 and Leu33–Glu36, folding into a larger compact region, Ile13–Ile39, by long range interactions, which are important for the receptor binding and EH activity. NMR spectroscopy is well known technique to provide 3-D structure of biomolecules in solution. However, unfortunately EH was found to be easy to aggregate at the concentration for NMR measurements.

Key words: Distance geometry; eclosion hormone; insecticide; NMR; restrained molecular dynamics; structure analysis.
*Corresponding author. Tel: +81-797-74-2594; Fax: +81-797-74-2598.
†Present address: Department of Polymer Science and Engineering, Kyoto Institute of Technology, Matsugasaki, Sakyo-ku, Kyoto 606, Japan.
‡Present address: Laboratory of Bio-signaling Chemistry, Department of Biotechnology, Ritsumeikan University, Noji, Kusatsu, 525 Japan.

0968-0896/98/$19.00
PII: S0968-0896(97)10049-9

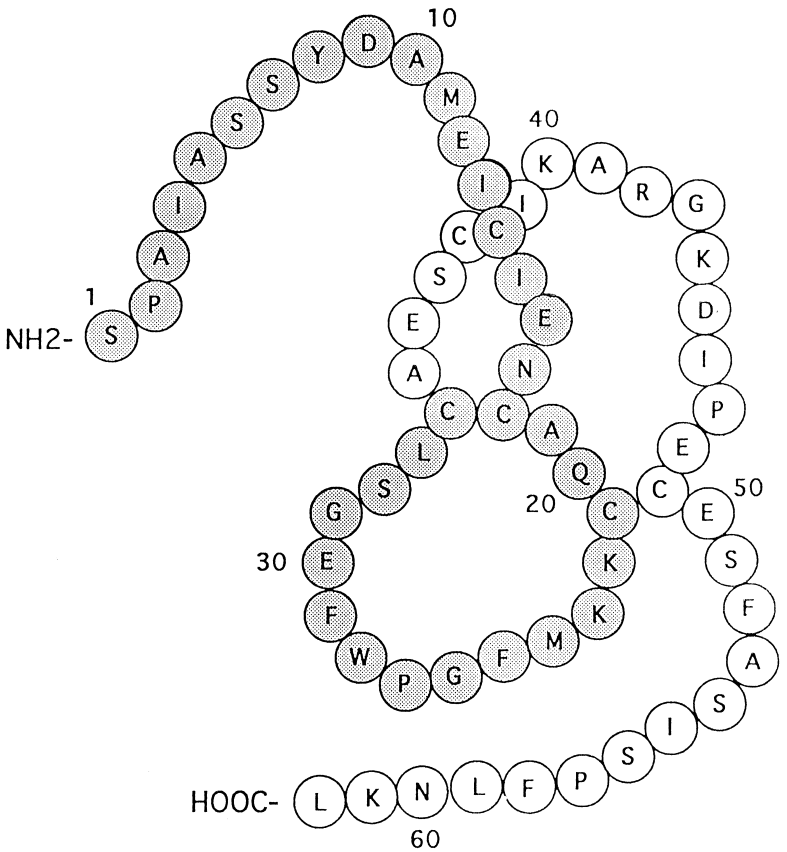

Figure 1. A schematic drawing of a main chain of *Bombyx mori* EH. The shaded region (Ser1–Cys34) indicates EH(1–34).

Therefore, this technique was not applicable for whole EH. As the final goal of the design of the inhibitor is the development of small lead compound, the strategy to synthesize fragments containing compact regions would be preferable. As a first step, we synthesized the N-terminal fragment (1–34) of eclosion hormone [EH(1–34)] which contains the predicted compact regions Asp9–Met24 and Trp28–Glu30 with one disulfide bridge (Cys18–Cys34) (Figure 1). The 3-D structure of the fragment (1–34) was elucidated in a mixed solvent system of 50% d_3-trifluoroethanol (TFE)/50% H_2O at pH 3 and 298 K by the combined use of NMR and distance geometry calculations and discussed in the relevance to the activity of the hormone.

Results

Circular dichroism (CD) measurements

CD spectra of EH(1–34) measured in H_2O, 50% MeOH/50% H_2O, and 50% TFE/50% H_2O together with that of whole EH in H_2O are shown in Figure 2. The CD spectrum of EH(1–34) in H_2O assumes no

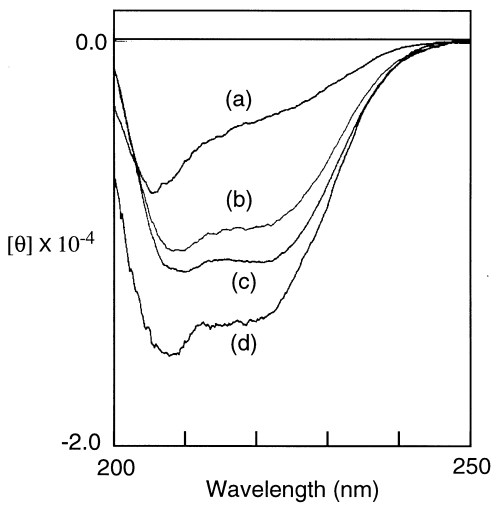

Figure 2. Circular dichroism spectra of (a) EH(1–34) in H_2O, (b) EH(1–34) in 50% MeOH/50% H_2O, (c) EH(1–34) in 50% TFE/50% H_2O, (d) EH in H_2O, recorded at pH 3 and 298 K. Peptide concentrations are 100 μM for (a), (b) and (c), and 50 μM for (d), respectively. The ellipticity units per mole of peptide residue (Θ) are given in deg cm^2 dmol^{-1}.

well-defined structure although whole EH shows a helical spectral pattern. On the other hand, EH(1–34) in 50% MeOH/50% H_2O, and 50% TFE/50% H_2O [denoted by the curves (b) and (c), respectively] showed negative peaks at 208 and 222 nm, indicating the presence of α-helical structure. Thus, the conformations of the fragment elucidated in mixed solvents are actually different from that in aqueous solution. However, the structure obtained in organic solvent such as TFE might reflect the real structural aspect in a hydrophobic environment such as the receptor binding site.

Although CD spectra can reveal overall characteristics of the secondary structure, no local information is available on the conformation of the fragment. To elucidate the 3-D structure, we measured the 2D NMR of the peptide.

^{1}H NMR assignments of the proton resonances and the secondary structure

The full resonance assignment of the proton NMR signals of EH(1–34) was performed using the sequential assignment procedure at pH 3 and 298 K in 50% d_3-TFE/50% H_2O solution.[16–18] Figure 3 shows the finger print region of NOESY spectrum of EH(1–34). The identification of amino acid spin systems was first established by means of direct and relayed through-bond connectivities (double-quantum filtered shift correlated spectroscopy (DQF-COSY) and homonuclear Hartmann–Hahn spectroscopy (HOHAHA)), followed by sequential resonance assignments using through-space nuclear Overhauser enhancement (NOE) connectivities. All the expected NH–CαH peaks were observed in the fingerprint region of DQF–COSY spectrum, and sequential NOE cross-peaks [typically, NH(i)–NH($i+1$), CαH(i)–NH($i+1$) and CβH(i)–NH($i+1$)] of nuclear Overhauser enhancement spectroscopy (NOESY) spectrum. Chemical shift values of all the resonances are listed in Table 1. The type and relative intensities of the sequential and medium range NOEs ($|i-j|<5$) are summarized in Figure 4. CαH(i)–NH($i+3$,4) and CαH(i)–CβH($i+3$) NOEs together with NH(i)–NH($i+1$) NOEs were observed in the residue range Ala10–Gln20. Thus, the peptide assumes an α-helix from residues 10 to 20, and other parts of the peptide would take rather extended conformation.

Three dimensional structures

One hundred and eighty constraints derived from NOESY spectra, and 18 coupling constants from DQF–COSY spectra were introduced in the distance geometry calculations. The distances which were obtained directly from the NOESY spectrum were used for the calculations employing the ratio with the referenced distance, such as the β–β″ distance. Starting from 100 initial structures with randomly chosen dihedral angles, the global minimum was searched by DIANA. The best 15 structures were subsequently refined by restrained energy

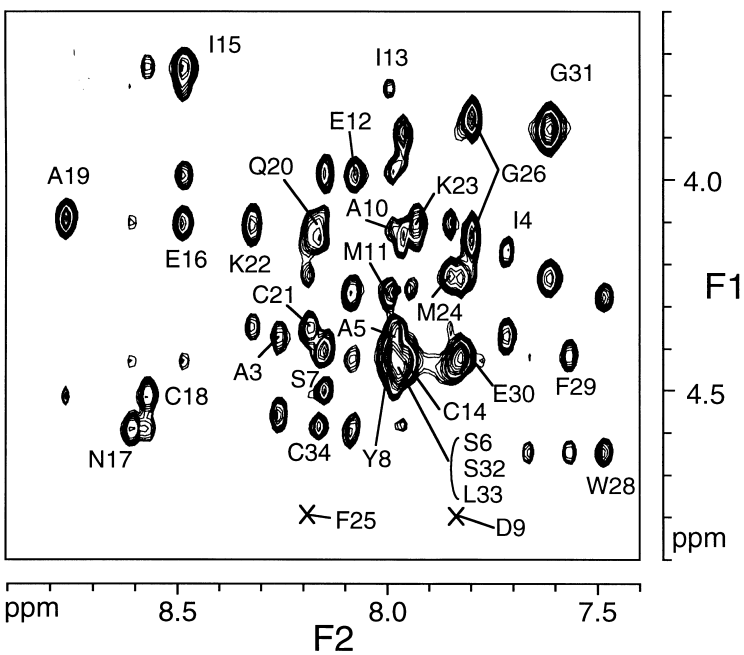

Figure 3. The finger print region of NOESY spectrum of EH(1–34) measured in 50% d_3-TFE/50% H_2O at 298 K, pH 3. The peptide concentration is 3.0 mM.

minimization (REM) and restrained molecular dynamics (RMD) simulations using the program XPLOR. Each structure was subjected to 50 steps of powell REM followed by 15 ps RMD simulations at 1000 K. The system was followed by 2.8 ps cooling steps to 300 K before 200 steps of REM were carried out. The time step used for the simulations was 2 fs and bond lengths were kept rigid by using the SHAKE algorithm. The force constants for the NOE distance constraints and dihedral angles were set to 50 kcal mol^{-1} Å^{-2}, and 50 kcal mol^{-1} rad^{-2}, respectively. Figure 5 shows a superposition overlay of the backbone atoms of all the residues. In this figure, the helical region was observed between Ala10 and Gln20. The root mean square deviation value calculated for the superposition of the final structures over the defined region from residue 10 to 20 for the backbone atoms was 0.88 ± 0.22 Å. Other regions of EH(1–34) would be flexible and lack significant stable structure.

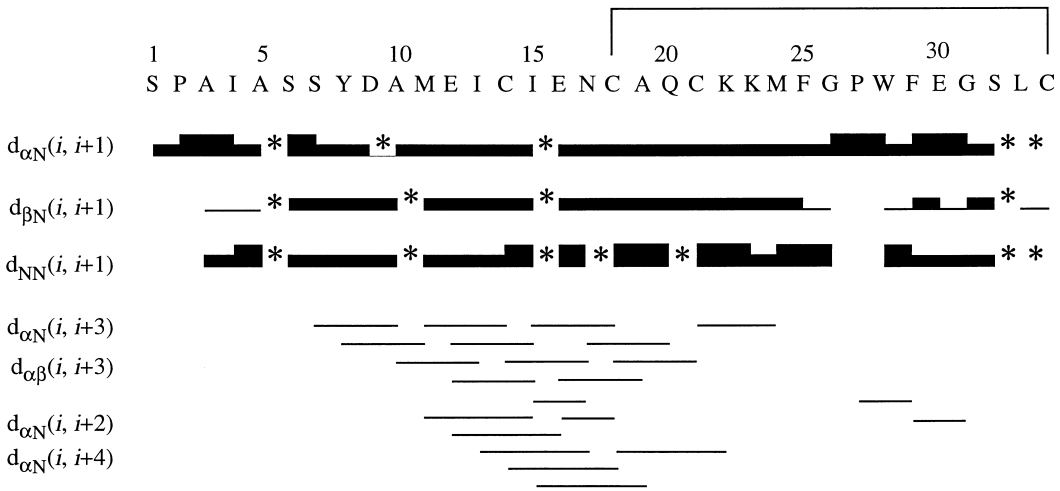

Figure 4. Summaries of NOE connectivities of the neighbouring residues. Terms d_{NN}, $d_{\alpha N}$ and $d_{\beta N}$ represent the sequential backbone connectivities. Intensities of the observed NOEs are represented by the thickness of the lines. An asterisk represents the region whose NOE intensities could not be obtained because of the signal overlap.

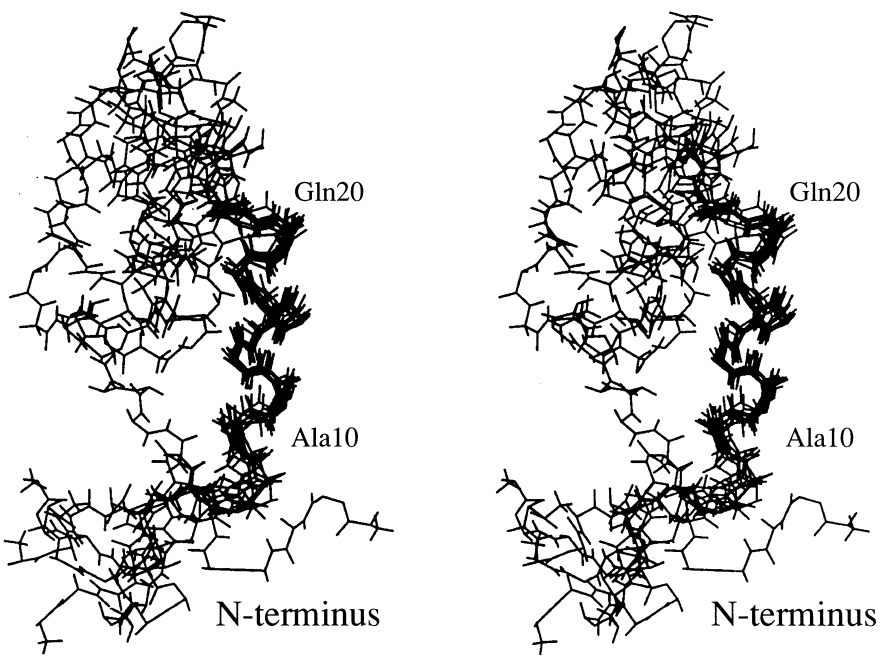

Figure 5. Three dimensional structures of EH(1–34) obtained by distance geometry and simulated annealing calculations.

Table 1. Resonance assignments for EH(1–34) protons in 50% TFE/50% H_2O solution

Position	Residue	NH	Hα	Hβ	Others
1	Ser	—	4.44	4.11	
2	Pro	—	4.56	2.44	γCH_2 2.01, 2.12, δCH2 3.70, 3.79
3	Ala	8.26	4.38	1.48	
4	Ile	7.72	4.18	1.95	γCH 1.27, γCH_3 1.00, δCH_3 1.00[a]
5	Ala	7.97	4.12	1.57	
6	Ser	7.98	4.41	3.99, 4.09	
7	Ser	8.16	4.40	3.96, 4.00	
8	Tyr	7.99	4.42	3.12, 3.14	H2,6 7.18, H3,5 6.85
9	Asp	7.84	4.75	3.17, 3.36	
10	Ala	7.98	4.35	1.50	
11	Met	7.99	4.26	2.03, 2.21	γCH_2 2.61, 2.70
12	Glu	8.08	3.98	2.15, 2.25	γCH_2 2.51
13	Ile	8.00	3.78	2.03	γCH 1.79, γCH_3 0.99, δCH_3 0.90
14	Cys[b]	7.95	4.44	3.26	
15	Ile	8.49	3.73	2.01	γCH 1.84, γCH_3 0.98, δCH_3 0.90
16	Glu	8.49	4.10	2.21, 2.31	γCH_2 2.53, 2.70
17	Asn	8.61	4.00	2.87, 3.14	δNH_2 6.52, 7.78
18	Cys	8.57	4.51	3.25, 3.42	
19	Ala	8.77	4.10	1.58	
20	Gln	8.17	4.15	2.31	γCH_2 2.55, εNH_2 6.67, 7.16
21	Cys[b]	8.18	4.35	3.18, 3.25	
22	Lys	8.33	4.11	1.86	γCH_2 1.46, 1.60, δCH_2 1.72, εCH_2 7.60[a]
23	Lys	7.93	4.10	1.96	γCH_2 1.46, 1.60, δCH_2 1.72, εCH_2 7.60[a]
24	Met	7.85	4.23	1.68, 1.86	γCH_2 2.27, 2.42
25	Phe	8.19	4.77	2.89	H2,6 7.16, H3,5 7.30, H4 7.22[a]
26	Gly	7.80	3.85, 4.14		
27	Pro	—	4.28	1.86, 2.10	γCH_2 1.55, 1.65, δCH_2 3.41, 3.50
28	Trp	7.49	4.65	3.31, 3.39	H2 7.19, H4 7.67, H5 7.21, H6 7.30 H7 7.55, NH 9.85
29	Phe	7.58	4.43	3.01	H2,6 7.16, H3,5 7.30, H4 7.22[a]
30	Glu	7.83	4.23	1.94, 2.14	γCH_2 2.40
31	Gly	7.62	3.90		
32	Ser	7.97	4.46	3.93	
33	Leu	7.98	4.43	1.71	γCH 1.71[a], δCH_3 0.91
34	Cys	8.17	4.58	2.91, 3.04	

[a]Approximate value.
[b]Acetoaminomethyl cysteine.

Bioactivity of the EH fragment

EH caused premature ecdysis behavior when injected into silkworm pharate adult at the dose of 0.1–0.2 ng/animal, while EH(1–34) did not cause the behavior even at the dose of 2 μg/animal. Co-injection of EH and EH(1–34), 0.2 ng and 2 μg/animal, respectively, showed the typical premature ecdysis, suggesting that EH(1–34) had no interaction with its receptor in the in vivo assay. Furthermore, we incubated the abdominal ganglia from silkworm pharate adults with EH(1–34), in the presence or absence of EH, and measured the activity of guanylate cyclase. As a result, EH(1–34) at the dose of 1 μM did not show any effect on the basal nor 1 nM EH-stimulated guanylate cycles, in vitro (data not shown).

Discussion

Kikuchi reported that biologically active sites in peptides are contained in the short range compact regions predicted by an average distance map (ADM).[19] The ADM for silkworm EH indicates the existence of the short range compact regions, Asp9–Met24, Trp28–Glu30 and Leu33–Glu36, folding into a larger compact regions, Ile13–Ile39, by long range interactions. They assumed that the relatively large short range compact region Asp9–Met24 of EH form α-helices, and the other smaller short range compact regions consisted of three or four residues are in β-turns.[14]

On the basis of the results obtained by site-directed mutagenesis, Kikuchi et al. suggested that the helical

structure around the 12th residue is required for the eclosion activity and Glu12 is important to keep the structure. Furthermore, Met24 is important to maintain the tertiary structure as well as to interact with a receptor, whereas Phe25 is likely to be required to construct a hydrophobic interaction inside the molecule to keep the active globular structure.

Present CD and NMR results indicated that N-terminal fragment EH(1–34) does not take any preferable conformations in aqueous solution. However, it assumes rigid conformations in mixed solvents which are considered to reflect the representative environment at a receptor site. In a recent study of actin peptides, it was shown that TFE stabilized α-helices only in regions with a propensity for α-helix formation.[20]

In fact, the CD spectrum of EH(1–34) in 50% TFE showed a typical helical pattern, while it showed a very weak one in H_2O. However, the CD spectrum of intact EH in H_2O showed a strong helical pattern which is similar to that of EH(1–34) in 50% MeOH. Probably, without a contribution by organic solvent, intact EH in H_2O can fold into a globular peptide in which a hydrophobic circumstance is created. Based on the equation of Chen et al., [21] nearly 30 residues of EH are involved in α-helical formation in H_2O. Since several residues at the C-terminal do not contribute to an intensity of the helical pattern of CD spectrum,[22] at least several residues in the 1–34 region should contribute to the helical formation. Thus, the conformation of EH(1–34) in 50% TFE is likely to reflect a physiological one which is induced by the hydrophobic solvent. Using the same equation described above, the helical content of EH(1–34) in 50% TFE was 35%, indicating that 12 residues are involved in the α-helix. On the other hand, our 3-D structure analyses of NMR spectra of EH(1–34) showed that the helical region is between 10 and 20, indicating that 11 residues are involved in the helix. Thus the numbers of residues in the possible helix of EH(1–34) are almost consistent in the two spectroanalyses.

The experimentally elucidated three dimensional structure of the fragment in a TFE aqueous solution by NMR is well consistent with the predicted one in terms of an α-helical region (Ala10–Gln20), although it is shorter than the predicted one (Asp9–Met24). However, we did not detect such a rigid conformation in the residue range of Trp28–Glu30 as predicted by Kikuchi et al. This part may be stabilized in the whole EH by interacting with the other part of the peptide[2,14] but not in the short fragment. Kikuchi pointed out that all of the Cys residues are on one side of the helix bound to other regions of the protein (i.e. they are interior residues), and that on the other hand, the polar amino acids, Glu12, Gln20, Lys23, and/or Asp9 are on the opposite side, which are exposed to solvent and thus potential receptor interaction.

Kikuchi reported that biologically active sites in peptides are contained in the short range compact region predicted by ADM. Although the EH(1–34) was proved to contain the compact region, it did not show any bioactivity in the in vivo nor in vitro assay. One possible explanation for the lack of biological activity in the fragment might be missing the carboxy terminal region (35–62). Recently, using site-directed mutageneses, Fujita and Maekawa identified several important residues in this region (unpublished results). These residues are involved in two small helices, one of which was predicted as a compact region with a long range interaction by ADM. These two helices are linked to the α-helix (12–22) by three disulfide bonds and also by a possible hydrophobic interaction between Phe25 and a residue near the C-terminal. Therefore, while EH(1–34) is not sufficient to show eclosion hormone activity, this fragment contains an important core region in which an α-helix exists and it plays a key role in constructing an active globular peptide. Further investigation of the three dimensional structures of longer fragments containing the predicted β-turn and other parts, and also their biological activity would provide more unequivocal information about the structure–activity relationship.

To develop the insecticide from the inhibitors of EH, the structural information about EH is essential. Unfortunately, native EH is easy to aggregate at the concentration for NMR measurement to elucidate the structure. And the most fragments synthesized in our laboratory so far had also several problems for NMR measurements. The fragment EH(1–34) studied here is the only one available for NMR measurements for the time being, although this fragment has neither EH-like activity nor inhibitory activity. Taking into account that there has been no experimentally elucidated structural information about EH to date, neither by X-ray nor NMR spectroscopy, the results that the fragment actually contains the compact region and that the structured region is smaller than that predicted by ADM must be useful information for the development of the design of the insecticide.

Conclusion

The structure elucidated for EH(1–34) is characterized by an α-helix in the N-terminal region (Ala10–Gln20) but no rigid structure was present from Cys21 through the C-terminus and for the N-terminal region (Ser1–Asp9). Thus, the present study experimentally revealed that EH(1–34) actually contains a predicted compact

region for EH which is considered to be crucial for hormone activity. The conformational feature may be responsible for the high binding affinity to the receptor. However, taking account of the lack of biological activity of the fragment, additional structural elements such as β-turn structure would be required for the full biological activity.

Experimental

CD measurements

The CD spectra were measured on a JASCO J600 spectro-polarimeter at 298 K in a quartz cell of 0.01 cm path length. All CD spectra were reported in terms of ellipticity units per mole of peptide residue. The concentrations of EH and EH(1–34) were 50 and 100 μM, respectively.

NMR measurements

For the measurements of NMR spectra, 5.6 mg of EH(1–34) was dissolved in 0.5 mL of 50% d_3-TFE/50% H_2O solution containing 0.01 M CD_3COOD. The peptide concentration was 3.0 mM. All proton NMR experiments were performed at 298 K on a Bruker AMX-600, and the derived data were processed on a Bruker X-32 computer with UXNMR software. 2-D DQF–COSY,[23] HOHAHA[24,25] and NOESY[26,27] spectra were acquired in the phase-sensitive mode by a time proportional phase incrementation method.[28] HOHAHA spectra with a MLEV17 spin lock sequence[29] were recorded with mixing times of 40 and 80 ms in order to identify further spin systems through chemical bond. Phase sensitive 2D NOESY spectra were recorded with mixing times of 100, 150 and 300 ms. NOESY data with a mixing time of 300 ms were used for sequential assignment, and those with the shorter mixing times were used for the estimation of the distances between protons. The data size was 2 K complex points for f_2 and 512 points for f_1 and repetition delay was 1.8 s. The f_1 and f_2 data were apodized with the squared sine-bell function and then Fourier transformed. The water OH resonance was suppressed by irradiation during the relaxation delay. 3-(Trimethylsilyl)propionate (TSP)-d_4 was used as an internal standard of chemical shift. The NMR analysis software FELIX (Biosym/MSI) was used for volume integration. Measurements of $^3J_{HN\alpha}$ coupling constants were obtained from well-digitized DQF–COSY spectrum.

Structure calculations

Distance constraints were derived from the NOESY spectra recorded with a 150 ms mixing time, which were classified as follows; very strong (2.5 Å), strong (3.0 Å), medium (3.5 Å), weak (4.0 Å) and very weak (4.5 Å). For restrained molecular dynamics calculations, the lower and upper bounds were defined as; very strong (−0.6 Å, +0.3 Å), strong (−1.2 Å, +0.3 Å), medium (−1.7 Å, +0.5 Å) and weak (−2.2 Å, +1.0 Å). The additional lower and/or upper bounds were applied in case of non-stereospecific assignments of methylene and methyl groups.[30] NOE intensities used as input for the distance geometry calculations were determined by integrating volumes for well-separated peaks and counting cross-peak contour levels for overlapped peaks.

The distance geometry calculations were performed with the DIANA program.[31] As for the first step of the program, 300 structures were generated with random dihedral angles uniformly distributed between −180° and +180°, and the target function was minimized according to the default minimizer from level 1 to 34. 32 structures with the smallest final target function value, out of the obtained 300 structures were chosen as starting structures for the restrained molecular dynamics calculation by the program XPLOR.[32,33] In order to refine the structures obtained by the distance geometry calculation, the following protocol was employed; 50 steps of a restrained energy minimization, followed by 15 ps, 7500 steps of a restrained molecular dynamics calculation (1000 K) with shake restraints to keep bond length fixed. Then the vdW force constant was increased gradually. Next, NOE potential function was changed to square well from asymptote, and constraint dihedral energy term was included. During the dynamics, the temperature was gradually decreased from 1000 K to 300 K by 25° steps. After the SHAKE restraint was reset, the last 200 steps of energy minimization were performed.

Graphical representation was carried out with the graphic program QUANTA (Biosym/MSI). All calculations and graphical representation were carried out on an IRIS 4D/35 computer.

Peptide synthesis

The eclosion hormone fragment (1–34) was chemically synthesized on an ABI 431A automated peptide synthesizer using Fmoc strategies.[14] The fragment contains one disulfide bridge (Cys18–Cys34) and other cysteine residues (Cys14 and Cys21) are protected by acetoaminomethyl groups.

Measurement of cGMP

Silkworm pupae were purchased from Katakura Industrial Co. Ltd. (Saitama, Japan). They were reared at

25° C with a 16 h-light and 8 h-dark photoperiod. Pharate adults were selected by their hatched antenna as a developmental marker and utilized for the bioassay.[34] Immuno assay kit (Yamasa) was used for the measurement of cGMP in silkworm abdominal ganglia. A pharate adult was dissected and abdominal ganglia were isolated. Several pupal ganglia were washed with insect saline and transferred into a tube containing Tris/Bis buffer pH 7.5 and mixed protease inhibitors. The reaction was started by adding EH(1–34), EH(1–34) plus EH or buffer into the incubation mixture and stopped by filtration. The ganglia were homogenized with 100 μL trichloroacetic acid solution and measured the content of cGMP as described in the attached protocol of the assay kit.

Acknowledgement

We thank Dr Kikuchi for stimulating discussion.

References

1. Truman, J. W. In *Molting and Metamorphosis*; Ohnishi, E.; Ishizaki, H., Eds.; Springer–Verlag: Berlin, 1990; pp 67–82.

2. Kono, T.; Nagasawa, M.; Isogai, H.; Fugo, H.; Suzuki, A. *Agric. Biolog. Chem.* **1987**, *51*, 2307.

3. Kataoka, H.; Troestschler, R. G.; Kramer, S. J.; Cesarin, B. J.; Schooley, D. A. *Biochem. Biophys. Res. Comm.* **1987**, *146*, 746.

4. Marti, T.; Takio, K.; Walsh, K. A.; Terzi, G.; Truman, J. W. *FEBS Lett.* **1987**, *219*, 415.

5. Kono, T.; Nagasawa, M.; Kataoka, S.; Fugo, H.; Suzuki, A. *FEBS Lett.* **1990**, *263*, 358.

6. Morton, D. B.; Giunta, M. *J. Neurochem.* **1992**, *59*, 1522.

7. Shibanaka, Y.; Hayashi, H.; Takai, M.; Fujita, N. *Eur. J. Biochem.* **1993**, *211*, 427.

8. Shibanaka, Y.; Hayashi, H.; Umemura, I.; Fujisawa, Y.; Okamoto, M.; Takai, M.; Fujita, N. *Biochem. Biophys. Res. Comm.* **1994**, *198*, 613.

9. Morton, D. B.; Simpson, P. J. *J. Comp. Physiol.* **1995**, *165*, 417.

10. Morton, D. B. *J. Neurobiol.* **1996**, *29*, 341.

11. Morton, D. B.; Truman, J. W. *J. Recpt. Signal. Transduct. Res.* **1995**, *15*, 773.

12. Truman, J. W. In *Comprehensive Insect Physiology Biochemistry and Pharmacology*; Kerkut, G.; Gilbert, L., Eds.; Pergamon: Oxford, 1987; Vol 8, pp 413–440.

13. Horodyski, F. M.; Ewer, J.; Riddiford, L.; Truman, J. W. *Eur. J. Biochem.* **1993**, *215*, 221.

14. Kikuchi, T.; Okamoto, M.; Geiser, M.; Schmitz, A.; Gohda, K.; Takai, M.; Morita, T.; Horii, K.; Fujita, N. *Protein Eng.* **1997**, *10*, 217.

15. Konishi, Y.; Frazier, R. B.; Olins, G. M.; Blehm, D. J.; Tjjoeng, F. S.; Zupec, M. E.; Whipple, D. E. In *Peptides, Chemistry and Biology*; Marshall, G. R., Ed.; Escom: Leiden, 1987; pp 479–481.

16. Wüthrich, K.; Billeter, M.; Braun, W. *J. Mol. Biol.* **1982**, *169*, 949.

17. Billeter, M.; Braun, W.; Wüthrich, K. *J. Mol. Biol.* **1982**, *153*, 321.

18. Wüthrich, K. *NMR of Proteins and Nucleic Acids*; John Wiley & Sons: New York, 1986.

19. Kikuchi, T. *J. Protein Chem.* **1992**, *11*, 579.

20. Sönnichsen, F. D.; Van Eyk, J. E.; Hodges, R. S.; Sykes, B. D. *Biochemistry* **1992**, *31*, 8790.

21. Chen, Y.; Yang, J. T.; Martinez, H. M. *Biochemistry* **1972**, *11*, 4120.

22. Grans, P. J.; Lyu, P. C.; Manning, M. C.; Woody, R. W. *Biopolymers* **1991**, *31*, 1605.

23. Rance, M.; Sørensen, O. W.; Bodenhausen, G.; Wagner, G.; Ernst, R. R.; Wüthrich, K. *Biochem. Biophys. Res. Commun.* **1983**, *117*, 479.

24. Braunschweiler, L.; Ernst, R. R. *J. Magn. Reson.* **1983**, *53*, 521.

25. Davis, D. G.; Bax, A. *J. Am. Chem. Soc.* **1985**, *107*, 2820.

26. Jeener, J.; Meier, B. H.; Bachman, P.; Ernst, R. R. *J. Chem. Phys.* **1979**, *71*, 4546.

27. Macura, S.; Huang, Y.; Suter, D.; Ernst, R. R. *J. Magn. Reson.* **1981**, *43*, 259.

28. Redfield, A.; Kunz, S. D. *J. Magn. Reson.* **1975**, *19*, 250.

29. Bax, A.; Davis, D. G. *J. Magn. Reson.* **1985**, *65*, 355.

30. Wüthrich, K. *Biochem. Biophys. Res. Commun.* **1983**, *117*, 479.

31. Güntert, P.; Braun, W.; Wüthrich, K. *J. Mol. Biol.* **1991**, *217*, 517.

32. Brünger, A. T.; Clore, G. M.; Gronenborn, A. M.; Karplus, M. *Proc. Natl. Acad. Sci. U.S.A.* **1986**, *83*, 3801.

33. Brünger, A. T. *J. Mol. Biol.* **1988**, *203*, 803.

34. Hayashi, H.; Shibanaka, Y.; Nakano, M.; Fujita, N. *Biochem. Biophys. Res. Comm.* **1990**, *173*, 1065.